Altitude Control of a Solar Balloon for Mars Exploration

Article *in* Advances in the Astronautical Sciences · January 2020

CITATIONS
0

READS
69

3 authors:

Tristan Schuler
The University of Arizona
9 PUBLICATIONS **6** CITATIONS
SEE PROFILE

Sergey Shkarayev
The University of Arizona
9 PUBLICATIONS **7** CITATIONS
SEE PROFILE

Jekan Thangavelautham
The University of Arizona
205 PUBLICATIONS **828** CITATIONS
SEE PROFILE

(Preprint) AAS 20-104

ALTITUDE CONTROL OF A SOLAR BALLOON FOR MARS EXPLORATION

Tristan Schuler,[1] Sergey Shkarayev[2], Jekan Thangavelautham[1]

Exploration of Mars has been made possible using a series of increasingly sophisticated landers, rovers and orbiters. These three options for exploration have operated for prolonged periods lasting months to years. However, due to limitations in landing technology, it is still not possible to access the rugged environments on Mars, particularly regions such as Valles Marineris, the southern highlands or the northern and southern poles. A solar balloon is a credible solution to accessing aerial imagery and performing science missions in previously hard to reach areas. Solar balloons are also heated naturally by the sun and don't require an external tank of gas for initial inflation. The present work analyzes the feasibility of solar balloons on Mars. The work presents an in-depth model for altitude control of a solar balloon and altitude controllability in the Martian atmosphere.

INTRODUCTION

Mars remains mysterious, with some important unsolved questions. One is the observation of Recurring Slope Lineae (RSL) that have formed at the edge of crater walls, canyons, cliffs and slopes. Initially they were hypothesized to be water flow, but the latest observations indicate potential for sand movement. Another is the seasonal observation of methane particularly near the bottom of canyons and cliff walls. These observations suggest the methane is originating from below ground. On Earth the principle source of methane is from biological processes. Could this suggest isolated microbial life in the Martian subsurface or a never-before encountered chemical reaction releasing methane? Furthermore, thanks to HiRise, there are series of intriguing formations and structures spotted from Martian orbit that could point to an early Mars that was wet and potentially habitable. A closer look at these ancient formations could provide concrete evidence, including remains of fossils.

To-date exploration of Mars has been made possible using a series of increasingly sophisticated landers, rovers and orbiters. These three options for exploration have operated for prolonged periods lasting months to years. However, due to limitations in landing technology, it is still not possible to access the rugged environments on Mars, particularly regions such as Valles Marineris, the southern highlands or the northern and southern poles.

A promising solution is to develop a solar balloon platform that travels with the wind and absorbs heat from solar radiation. Solar balloons are not a new concept but have not been flown on Mars yet. Solar balloons eliminate the need for carrying tank of a "lighter-than-air" gas and heat up naturally from solar radiation by utilizing a lightweight material with a high absorptivity and

[1] Space and Terrestrial Robotic Exploration (SpaceTREx) Laboratory, Aerospace and Mechanical Engineering Department, University of Arizona
[2] Micro-Air Vehicles Laboratory, Aerospace and Mechanical Engineering Department, University of Arizona

low emissivity. Leaks are also not an issue unless massive tears in the envelope occur. This paper explores the feasibility of a solar balloon platform for Mars, demonstrates a model for predicting altitude trajectories in the Martian atmosphere, and explores the controllability of the system by adjusting several parameters.

The following sections explore the feasibility of deploying a solar balloon on Mars for exploration and introduce a basic design concept that could fit in a CubeSat sized payload. A Mars radiation model based on latitude, time of day, and elevation is presented as well as the heat transfer to heat the ambient atmospheric air inside the balloon to produce buoyancy. Additionally, altitude control of the balloon is demonstrated by opening and closing a vent on the top side of the balloon.

RELATED WORK

There have been several proposals for various types of extreme-exploration vehicles on Mars. The NASA JPL Mars helicopter will be launching with the Mars 2020 rover and can fly for around 90 seconds on Mars to capture aerial imagery.[1] This helicopter is meant to work in conjunction with the rover to provide better path planning. Similarly, the Dragonfly mission headed by JHU APL, another extraterrestrial rotorcraft platform has been proposed to explore Titan.[2]

Besides rotorcraft, planes have also been proposed to explore other planets. Several Mars aircraft that have been proposed by NASA include Kitty Hawk, AME, and MAGE.[3] These designs all required a propulsion source. Recently, an inflatable sail plane has been proposed to fly long distances in the Martian Atmosphere using dynamic soaring and riding the wind currents. [4]

There have been a few proposals for solar balloons on Mars and there have been a few terrestrial experiments at high altitudes that mimic Martian conditions. [5] [6] [7] [8] Super-pressure airships have also been proposed for exploring Mars.[9] [10] The potential issue with super-pressure balloons is that they are susceptible to leaks and they also require an external tank of gas for initial deployment before flying. However, lighter than air balloons have flown on another planet before; NASA's VEGA mission launched 2 balloons into the atmosphere of Venus.[11] These helium-filled balloons were not controlled and stayed at an equilibrium altitude. Titan is another area of high interest for ballooning missions.[12] [13]

System Design

The solar balloon will have an envelope constructed out of an extremely lightweight mylar-like material that has a high absorptivity in the visual spectrum and a low emissivity in the infrared spectrum to convert the most sunlight to heat. The solar balloon will be similar in volume to a hot air balloon but will lift a significantly lighter payload due to the low atmospheric pressure on Mars.

For initial deployment of the balloon, the balloon will "piggyback" on a larger Mars mission and be deployed from an EDL vehicle. While in the upper atmosphere, the stowed balloon payload will use propulsion to separate from the main vehicle and then unravel the envelope and deploy a break away parachute. Once the envelope is unraveled, a hoop at the bottom of the balloon will open to allow air intake into the balloon as it's rapidly descending. The parachute will ensure that the balloon is in the right position for air to enter the inside of the envelope. From the model discussed in the next few sections, the balloon should reach a hot enough temperature to achieve buoyancy before reaching the ground. The solar balloon will then autonomously be selecting an area for soft landing for the night. Once the sun rises again, the balloon will fly again and continue

exploring and conducting science missions. Figure 1 shows the deployment of the balloon in the Martian atmosphere.

Figure 1. Initial Balloon Deployment from EDL Vehicle. Image Courtesey of NASA.

Additionally, the balloon will have a vent at the top for altitude control. The vent is a step input of either open or closed and will be radio controlled from the gondola. A gondola will be connected to the balloon hoop and contains the flight controller, anchor system, solar panels, and any additional sensors for science missions. Depending on payload weight and envelope size the balloon could potentially fit in a 6U CubeSat. A gondola with only the essentials should be able to fit in less space than a 4U. Figure 2 shows a basic design concept for the stowed balloon.

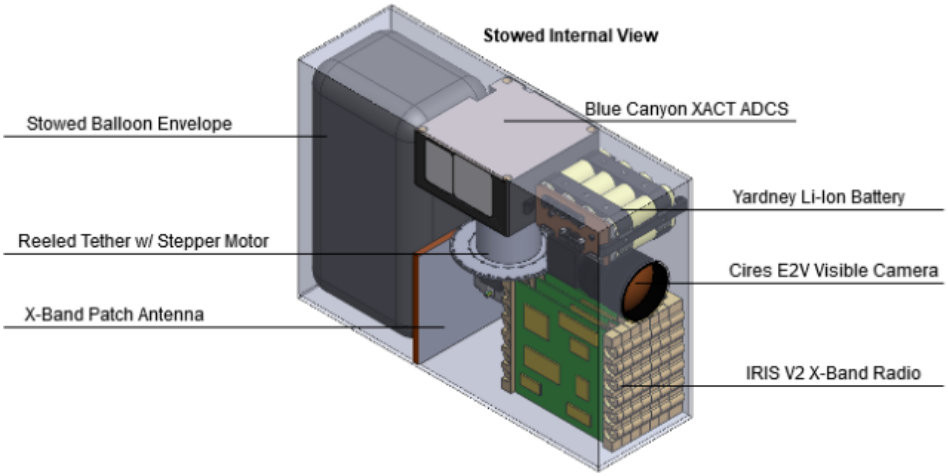

Figure 2. Stowed Internal view of a 6U CubeSat Deployed Solar Balloon

The solar balloon will explore Mars by flying along with wind currents. The vent will allow the balloon to rise and fall in the atmosphere to enter different wind currents and control its path, to an extent. The MAVEN spacecraft has taken wind measurements in the upper atmosphere during different seasons suggesting that wind currents vary across the planet and change with the seasons.[14] Wind measurements were also taken locally over 60 Martian days at the Viking Lander site.[15] Wind speeds recorded typically between 2-7 m/s during the summer, 5-10 m/s in the fall, and up to

30 m/s during dust storms. The local wind direction also varied at different times during the day, sometimes over 130º.

These observations are promising for using wind currents to control solar balloons on Mars. If different elevations don't have varying wind currents, the direction changes frequently enough from day to day to reach new areas of interest. Additionally, the long-term current direction changes open up the opportunity for full planet exploration with long duration missions. Figure 3 shows how the NASA Ames Mars Global Climate Model can be used to get estimates of seasonal wind patterns from target landing site to exploration site for the solar balloon.

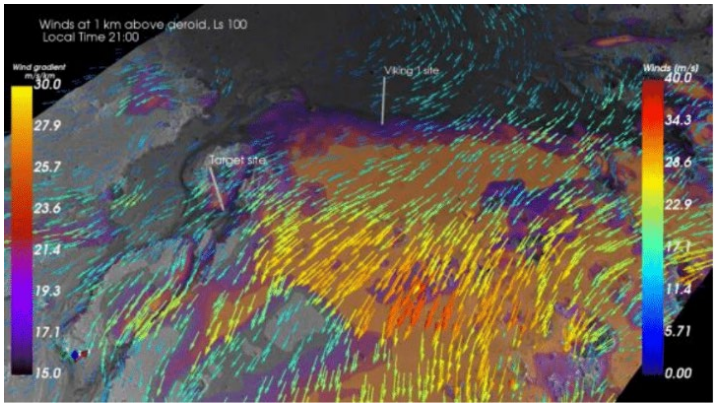

Figure 1. Estimate of Wind Pattern Using NASA Ames Mars Global Climate Model

MARTIAN RADIATION MODEL

The following Martian radiation model is used to calculate the feasibility of solar balloons on Mars. The solar balloon used solar radiation to absorb heat and generate lift. This model is also used to determine flight time, range, and flight capabilities.

Most of the relevant equations used for creating this Martian solar balloon model are taken from a combination of two sources. NASA provided equations for their Balloon Ascent Trajectory software package designed for predicting trajectories of super-pressure balloons on Earth.[16] Additionally, a radiation model for Mars is from NASA is used to predict solar radiation intensity at different locations and conditions on Mars.[17]

Direct Solar Radiation

Direct solar irradiance at the top of the Martian atmosphere is given by:

$$I_{sun,0} = 590 * \frac{1 + e * \cos(L_s - 248)^2}{(1 - e^2)^2} \quad (1)$$

Solar declination is given by:

$$\delta = \sin(24.936) * \sin(L_s) \quad (2)$$

where 24.936º is the Mars obliquity of rotation axis.

The solar zenith angle at any time of day is given by:

$$z = \arccos(\sin(\phi) * \sin(\delta) + \cos(\phi) * \cos(\delta) * \cos(\omega)) \quad (3)$$

where ϕ is the latitude, and ω is the solar hour angle.

$$I_{Sun} = G_{sun,0} * \cos(z) * \frac{f(z,\tau)}{0.9} \tag{4}$$

where $f(z,\tau)$ can be interpolated from Table IV of Applebaum.[17]

Reflected Sunlight

Additionally, reflected sunlight from the atmosphere contributes to heating the balloon envelope. This can be measured with the albedo flux.

$$q_{albedo} = Albedo * I_{Sun} * sin(z) \tag{5}$$

IR Radiation

Infrared Diffuse flux from the ground:

$$I_{\{IR,0\}} = \epsilon_{\{Mars\}} * \sigma * T^4_{\{ground\}} \tag{6}$$

Infrared flux from the ground varies with atmospheric pressure where the transmissivity is:

$$\tau_{atm} = 1.716 - 0.5 * \left[\exp\left(-0.65 * \frac{P_{air}}{P_0}\right) - \exp\left(-0.95 * \frac{P_{air}}{P_0}\right)\right] \tag{7}$$

The diffuse IR flux from the ground is then denoted by:

$$q_{IR} = I_{IR,0} * \tau_{atm} \tag{8}$$

Effective Area for a Spherical Balloon

For the baseline balloon model, the shape of the balloon is assumed to be a sphere.

For heat loss to the environment the entire surface area is used:

$$A_{surf} = \pi * d^2 \tag{9}$$

For direct solar radiation the projected area for a sphere is used:

$$A_{proj} = 0.25 * \pi * d^2 \tag{10}$$

For reflected sunlight from the Martian surface, the view factor of the planet surface for a sphere is used:

$$ViewFactor = \frac{1 - \cos\left(HalfCone_{angle}\right)}{2} \tag{11}$$

where the half cone angle is denoted by:

$$HalfCone_{angle} = \arcsin\left(\frac{R_{Mars}}{R_{Mars} + z}\right) \tag{12}$$

Total Radiant Heat Load on Balloon Envelope

The individual heat fluxes are multiplied by their corresponding effective areas to determine the total radiant heat load on the balloon envelope. The absorptivity in the infrared spectrum, α_{IR}, is assumed to be equivalent to the emissivity, ϵ.

Absorbed direct sunlight is denoted by:

$$Q_{sun} = \alpha * A_{proj} * q_{Sun} \tag{13}$$

Absorbed Albedo Heat is denoted by:

$$Q_{Albedo} = \alpha * A_{surf} * q_{Albedo} * ViewFactor \tag{14}$$

Absorbed Martian Surface IR Heat is denoted by:

$$Q_{IR,Surface} = \alpha_{IR} * A_{surf} * q_{IR,Surface} * ViewFactor \tag{15}$$

Emitted IR Energy from the Envelope is denoted by:

$$Q_{IR,emit} = \sigma * \epsilon * A_{surf} * T_{envelope}^4 \tag{16}$$

The overall heat radiation on the balloon is then denoted by:

$$Q_{rad} = Q_{sun} + Q_{Albedo} + Q_{IR,Surface} - Q_{IR,emit} \tag{17}$$

Figure 4 shows the different effects of radiation throughout the day and Figure 5 shows the total radiation available throughout the day as a function of elevation.

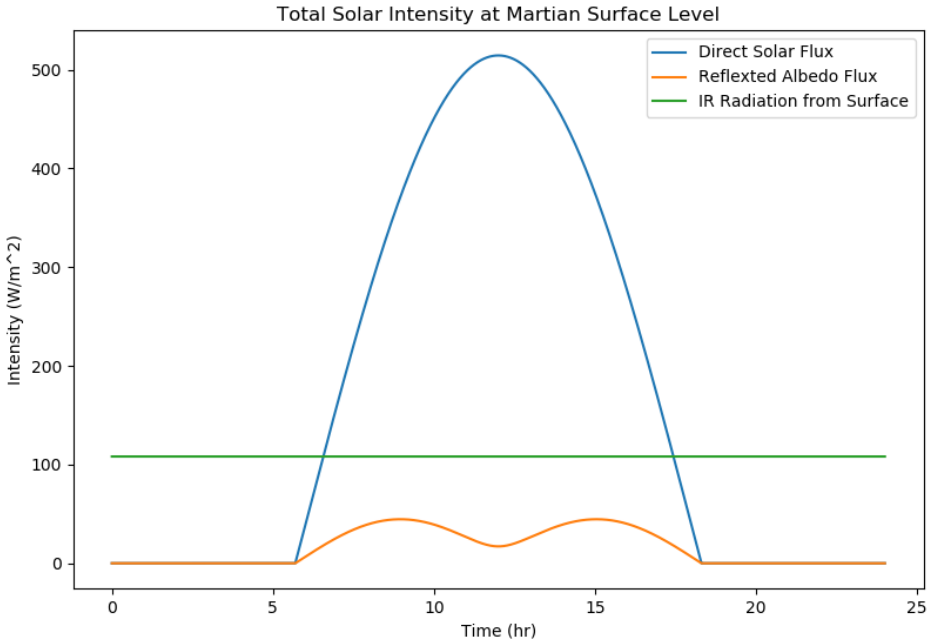

Figure 2. Total available radiation throughout Martian Day at surface Level

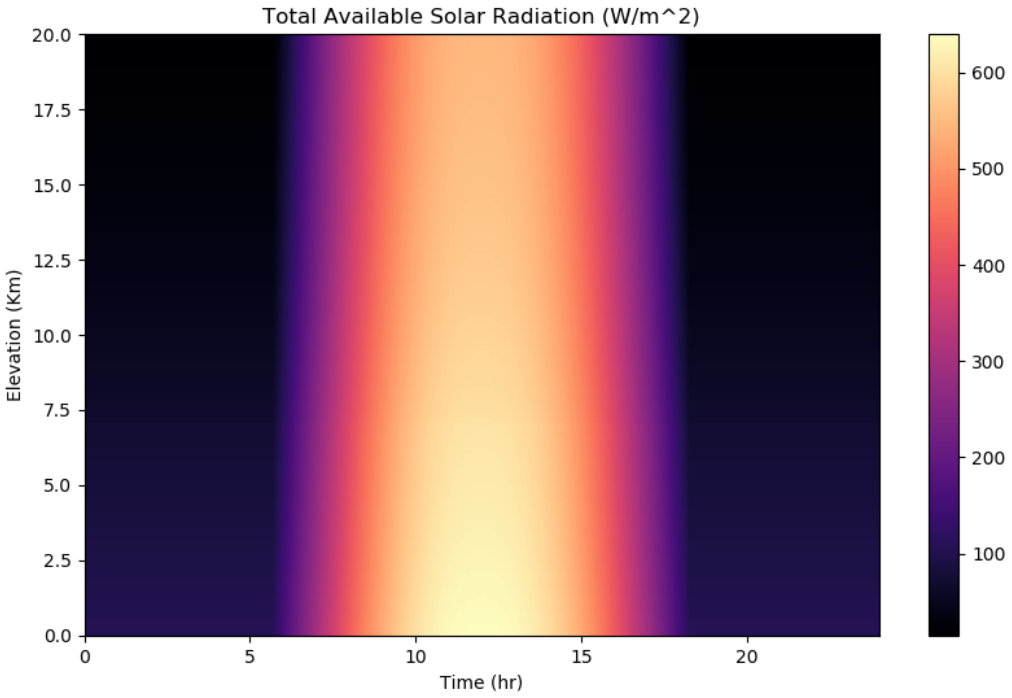

Figure 3. Total Available Radiation as a function of Elevation and TOD on Mars

CONVECTIVE HEAT LOADS ON BALLOON

External Free Convection

External free convection on the balloon envelope is a function of the dimensionless Nusselt Number which is a function of the dimensionless Grashoff number.

$$Gr_{CO^2,Ext} = \frac{\rho_{air}^2 * g * \left|T_{envelope} - T_{atm}\right| * d^3}{T_{atm} * \mu_{CO^2}} \tag{18}$$

Dimensionless Nusselt number for a sphere in free convection:

$$Nu_{CO^2} = 2 + 0.45 * (Gr_{CO^2} * Pr_{CO^2})^{0.25} \tag{19}$$

Free convection heat transfer coefficient for the balloon envelope:

$$h_{free} = \frac{Nu_{CO^2} * k_{CO^2}}{d} \tag{20}$$

External Forced Convection

The balloon also experiences external forced convection due to buoyancy and relative air movement. The heat transfer coefficient for external convection due to natural buoyancy is denoted by:

$$h_{ext,forced} = \frac{k_{CO^2}}{d} * (2 + 0.41 * Re^{0.55}) \tag{21}$$

where Re is the Reynolds number denoted by:

$$Re = \frac{U * d * \rho_{CO^2}}{\mu_{CO^2}} \tag{22}$$

Due to the balloon traveling with the wind, forced convection due to the wind is not modeled. With an anchoring system however, forced convection due to wind will need to be considered. The external heat convection is the denoted by:

$$Q_{conv,ext} = h_{free} * A_{surf} * \left(T_{atm} - T_{envelope}\right) \tag{23}$$

Where the maximum heat transfer coefficient is used between free and force convection.

Internal Free Convection

The free convection heat transfer coefficient for the inside of a sphere is:

$$h_{internal} = 0.13 * k_{CO^2} * \left(\frac{\rho_{air}^2 * g * \left|T_{envelope} - T_{CO^2,int}\right| * Pr_{CO^2}}{T_{CO^2,int} * \mu_{CO^2}}\right)^{\frac{1}{3}} \tag{24}$$

The internal free convection in then denoted by:

$$Q_{conv,int} = h_{internal} * A_{surf} * \left(T_{envelope} - T_{CO^2}\right) \tag{25}$$

Venting

The only input for controlling the solar balloon is a vent at the top of the balloon. For this model, the vent acts as a step input varying the mass flow rate of hot air leaving the balloon. An assumption for heat loss due to venting is that the volume of the balloon is not affected.

$$Q_{vent} = \dot{m} * (T_i - T_{atm}) \tag{26}$$

TRAJECTORY EQUATIONS

The following differential equations combine all the previous equations to calculate the change in temperature and buoyancy of the solar balloon throughout the day. Figure 6 shows the heat transfer loads on the balloon.

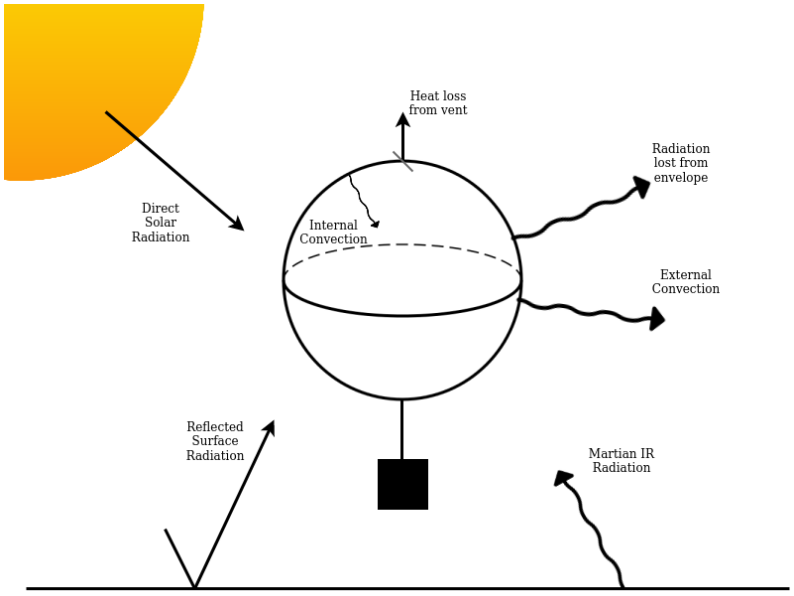

Figure 4. Heat Transfer Sources on Solar Balloon

Heat Transfer

The change in the surface temperature of the balloon envelope and the internal gas are found by equations (27) and (28) respectively:

$$\frac{dT_s}{dt} = \frac{\dot{Q_{rad}} + \dot{Q_{conv,ext}} - \dot{Q_{conv,int}}}{c_{v,env} * m_{envelope}} \tag{27}$$

$$\frac{dT_i}{dt} = \frac{\dot{Q_{conv,int}} - \dot{Q_{vent}}}{c_{v,CO^2} * m_{CO^2}} \tag{28}$$

Velocity and Acceleration

The buoyancy force is denoted by:

$$F_b = (\rho_{atm} - \rho_{int}) * V_{bal} * g \tag{29}$$

The drag force is denoted by:

$$F_d = .5 * C_d * rho_{atm} * U^2 * A_{proj} \tag{30}$$

where U is the velocity of the balloon, and C_d is the coefficient of drag .

Force due to gravity is denoted by:

$$F_g = \left(m_{payload} + m_{envelope}\right) * g \tag{31}$$

The vertical acceleration of the balloon is denoted by:

$$\frac{d^2z}{dt^2} = \frac{dU}{dt} = \frac{F_b - F_g - F_d}{m_{virtual}} \tag{32}$$

Where the virtual mass is the total mass of the balloon system:

$$m_{virt} = m_{payload} + m_{envelope} + C_{virt} * \rho_{atm} * V_{bal} \tag{33}$$

ANALYSIS

Table 1 shows the assumptions for a baseline balloon model on Mars that can lift a 10kg payload. Mars Atmospheric properties are taken from NASA[17] and material properties are from solar balloon research done by JPL[6]. The material is a germanium aluminum alloy that weighs 9 g/m^2.

Table 1. Assumptions for Baseline Balloon Model

*Dynamic Viscosity, μ	\$1.130*10^{-5} (N s/m^2)
*Thermal Conductivity, k	\$10.024*10^{-3} (W/m ºK)
*Prandtl Number, Pr	0.76

Diameter, d	18 (m)
Payload Mass, $m_{payload}$	5 (kg)
Envelope Density	.009 (kg/m^2)
Envelope Emissivity, ϵ	.003
Envelope Absorptivity, α	0.6
Envelope Specific Heat Capacity, c_v	320 $(J/kg\ ^\circ K)$
Coefficient of Drag, C_d	0.5
Mars Surface Temperature	225 (ºK)
Ground Emissivity	0.95
Mars Albedo	0.17

*Due to very low atmospheric temperature and temperature on Mars, these values are assumed to be constant.

Altitude Trajectory Without Control Input

The balloon trajectory follows a cycle where the balloon temperature cools down to slightly above ambient temperature during the night and then quickly heats up and cools off throughout the day as the sun rises and sets. Figure 7 and Figure 8 show the temperature profile of the baseline balloon model over a two-day period and the resulting trajectory with no control input. The internal temperature lags the heating of the surface because the thermal mass of the ambient air is much higher than the balloon material. For the baseline balloon model, once the air inside the balloon reaches an internal temperature of about 340ºK, the balloon begins to accelerate upwards. Another result from this model is that the envelope heats up fast enough for the balloon to achieve buoyancy before hitting the ground after initial deployment in the Martian atmosphere.

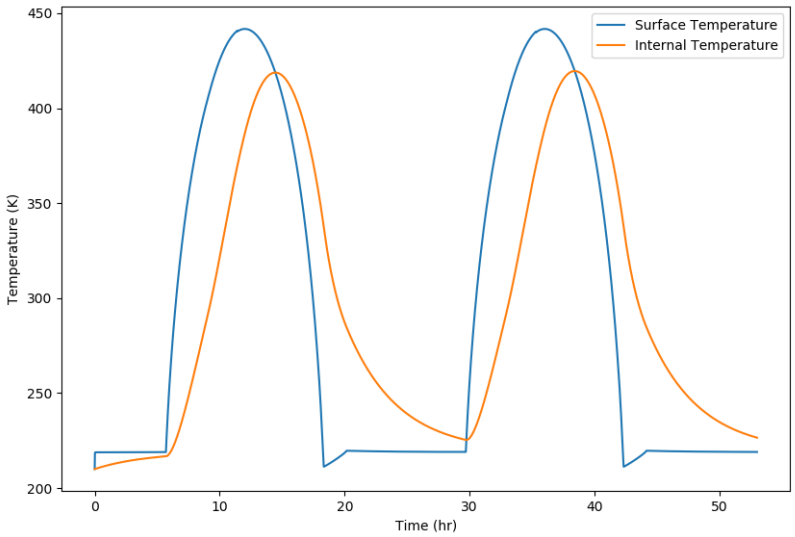

Figure 5. Temperature Model for Baseline Balloon Model Over 2-Day Period Without Control Input

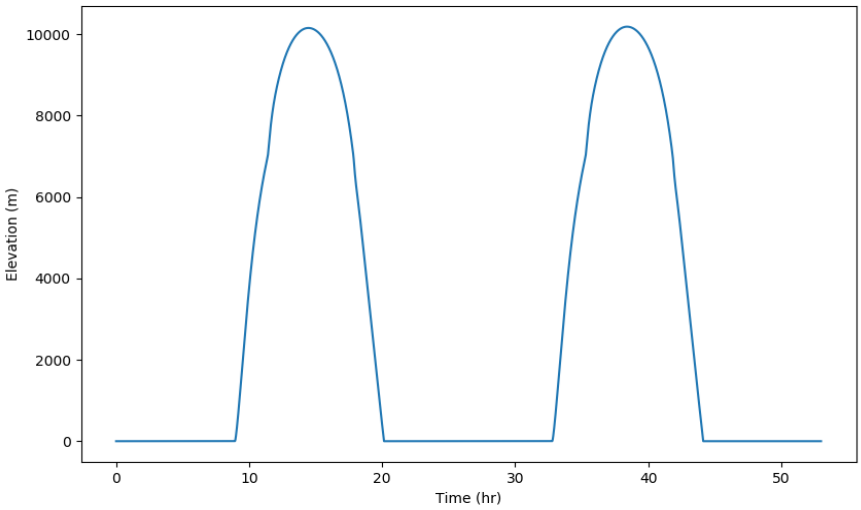

Figure 6. Elevation Trajectory for Baseline Balloon Model Over 2-Day Period Without Venting

Altitude Feedback Control

From Martian hours 9 to 15, the temperature of the balloon envelope stays within a range of approximately 35ºK and the internal temperature of the balloon reaches a temperature where altitude control via venting is possible. Depending on the size of the balloon and mass of the payload, different elevations can be reached and maintained. Because the temperature is constantly changing throughout the day due to the sun's position and changes in elevation, the balloon will never reach a steady altitude for an extended period of time and will have to perform venting actions to maintain a desired altitude. Venting results in a slow oscillation about a desired set point. Figure 9 shows position-only altitude control for the baseline balloon model at various vent mass flow rates. As mass flow rate increases, the number of vent opening and closing actions decreases but the error about the setpoint increases.

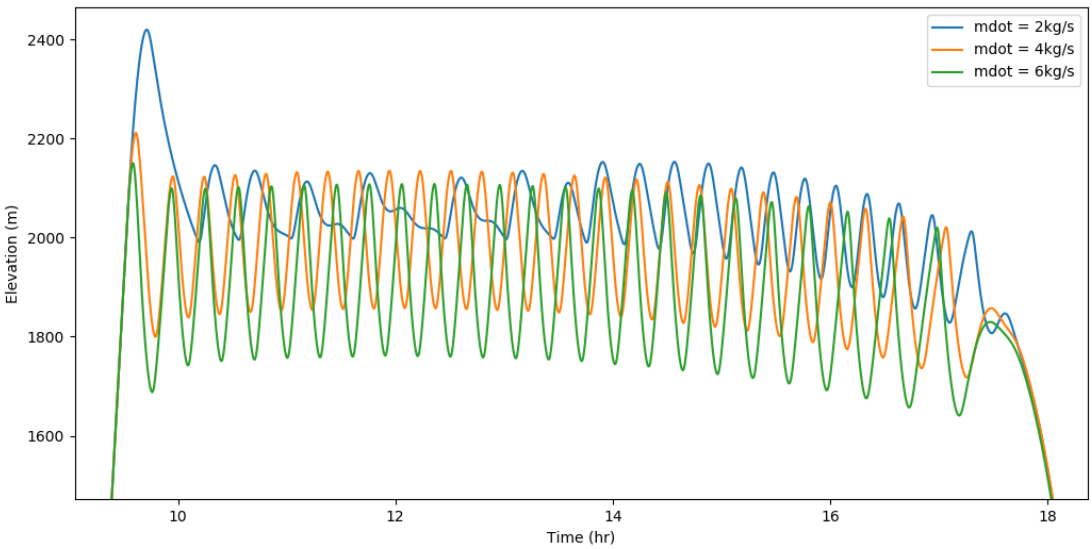

Figure 7. Altitude Position-Only Control for Different Vent Mass Flow Rates

An alternative to using position-only control is a combination of feedback control on position and velocity. A velocity controller decreases the percent overshoot and maintains an altitude with less error during oscillations. Figure 10 shows a comparison between a position controller with a vent mass flow rate of 2.2 kg/s and a velocity controller with a mass flow rate of 12 kg/s. These mass flow rates were chosen as an example because the average position about the setpoint was approximately the same for each type of controller during the hottest part of the day.

Figure 10 also introduces the idea of "dead zones" which helps the feedback controller maintain an average position closer to the desired setpoint. For position control and at lower mass flow rates, the dead zone should be below the desired setpoint because the cooling of air inside the balloon is a slower process. For velocity control, a much larger mass flow rate can be used, and the vent is open for a much shorter amount of time, resulting in a dead zone above the desired setpoint. The balloon continues to fall after the vent is closed until the balloon reaches a temperature that is hot enough to achieve neutral buoyancy. Mass flowrates, maximum velocities, and dead zones all change depending on the desired altitude, payload, and size of the balloon.

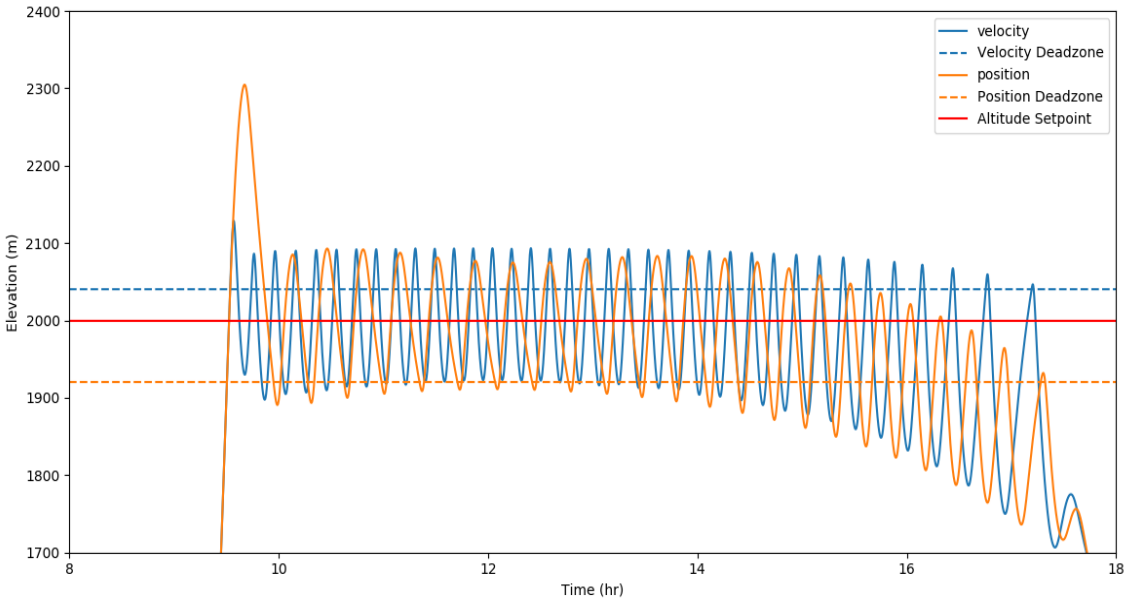

Figure 8. Position vs Position-Velocity Controller for Base line Balloon Model Maintaining an Altitude of 2km

Table 2. Altitude Control at Various Elevations and Payloads

Setpoint (m)	Payload (kg)	Vent Opens	Dead zone (m)	$\dot{m}$ (kg/s)	+/- v (m/s)	Stable Time (hr)	Vent Opens/hr
2000	0	80	-30	12	+.55/-.60	6	13
2000	5	58	+40	12	+.15/-.10	5.5	10.5
2000	10	30	+50	5	+.05/-.10	3.5	8.5
5000	0	80	+20	12	+.45/-.40	6	13
5000	5	48	+50	7	+.15/-.10	4.5	10.5
5000	10	-	-	-	-	-	-

Table 2 shows a trend between altitude setpoint, and payload for a position-velocity controller. There are several parameters that can be changed for maintaining altitude. The parameters that have the most effect are mass flow rate of the vent and the mass of payload. These samples are for oscillations between +/-100m of the desired set point. A lower mass flow rate leads to less error in maintaining a desired set point but requires more venting, which requires more power, and more wear and tear on the balloon system. Additionally, heavier payloads require less mass flow rate from the vent to let colder air in because the balloon accelerates downwards quicker due to gravity. A third trend is that when a higher stabilization altitude is desired, less mass flow rate is needed to maintain an altitude within +/-100m because the atmospheric pressure is lower, and in effect results in a lower ΔT required to lose buoyancy. Depending on balloon size and the payload mass, some altitudes are not reachable, as shown by the baseline balloon with a 10kg payload attempting to reach an altitude of 5000m. Selecting all these parameters will be highly mission specific and an interesting optimization problem.

Multi-Day Missions

At the end of each day as the sun begins to set, the solar balloon envelope rapidly drops in temperature which also drops the internal atmospheric air inside the balloon. The balloon deploys on the first flight by filling up with air during initial entry and descent. In order to fly a second day, the balloon has to fill up with air again after resting on the surface for a night, which presents some challenge.

There are three different solutions to ensure the balloon can fly additional days. One option is to have a propeller system, or dragging robot mechanism, that allow the balloon to fill back up in the morning with ambient air during sunrise. Another option is to have a heat generation source that keeps the air inside the balloon warm enough to remain buoyant enough to lift the envelope, but not necessarily buoyant enough to lift the payload. The final option is to have the balloon turn rigid during the initial flight from ultraviolet curing so that the envelope maintains it's shape even when the air isn't warm enough to produce lift.

Significance

This model demonstrates that solar balloons are a feasible platform for exploring on Mars. The balloons can explore greater distance much faster than a rover and capture aerial imagery as well as perform other science missions with different types of sensor payloads. The balloons will also be able to explore previously inaccessible areas such as crater and cliff walls.

Additionally, the balloons can be used as a platform to deploy other smaller platforms. One possibility is to carry inflatable Mars sailplanes.[4] The sailplanes can travel long distances much faster than balloons but require a method for deploying from the atmosphere again if multi-flight missions are desired. Small explorations robots, such as SphereX could be deployed as well. [18] SphereX conducts long duration hops interspersed with short flights and thrives in low gravity conditions. Another possibility is deploying a pseudolite network for multi agent robot systems in order to do localization.[19]

CONCLUSION

This paper explores the feasibility of a solar balloon for exploration on Mars and provides a detailed model for predicting the trajectory of the balloon. The vertical controllability of the balloon was explored using two variations of feedback control and adjusting parameters to achieve better results. Follow-up work will focus on experimental validation of the attitude control methods identified. In the event of a Martian solar balloon mission, engineers can build off of this model to help

design a balloon for Mars and adjust the balloon size, payload mass, and control parameters for a specific mission in the Martian atmosphere.

ACKNOWLEDGMENTS

The authors would like to acknowledge Leonard Dean Vance for his help with developing this Martian solar balloon model.

NOTATION

e	Orbital Eccentricity
L_s	Areocentric Longitude
ϕ	Latitude
τ	Optical Depth
δ	Solar Declination
ω	Solar Hour Angle
z	Zenith Angle
d	Diameter (m)
α	Absorptivity, visible light
ϵ	Emissivity, IR
g	Acceleration due to gravity (m/s^2)
k_{CO^2}	Thermal Conductivity of CO^2 (W/m ºK)
mu_{CO^2}	Dynamic Viscosity of CO^2 (N s/m^2

[1] Balaram, Bob, et al. "Mars helicopter technology demonstrator." *2018 AIAA Atmospheric Flight Mechanics Conference*. 2018.

[2] E.P. Turtle, et al., "Dragonfly: In-Situ Exploration of Titan's Organic Chemistry and Habitability," 49th Lunar and Planetary Science Conferencem, 1641, 2018

[3] M. Hassanalian, D. Rice, and A. Abdelkefi, Evolution of Space Drones for Planetary Exploration: A Review, Progress in Aerospace Sciences, 2018.

[4] Bouskela, Adrien, et al. "Attitude Control of an Inflatable Sailplane for Mars Exploration." *arXiv preprint arXiv:1902.02083* (2019).

[5] Jones, J., et al. "Montgolfiere balloon aerobots for planetary atmospheres." International Balloon Technology Conference. 1997

[6] Jones, Jack, and Jiunn Wu. "Solar montgolfiere balloons for Mars." *International Balloon Technology Conference*. 1999.

[7] Jones, J., Fairbrother, D., Lemieux, A., Lachenmeier, T., and Zubrin, R., “Wind-driven Montgolfiere Balloons for Exploring or Landing on Mars,” 43rd AIAA Aerospace Sciences Meeting and Exhibit, 2005, p. 844.

[8] Bowman, D. C., Norman, P. E., and Yang, X., “Solar balloons: A low cost, multi-hour flight system for the lower stratosphere,” 2015.

[9] Girerd, Andre, and Andre Girerd. "A case for a robotic Martian airship." *12th Lighter-Than-Air Systems Technology Conference*. 1997.

[10] Kerzhanovich, V. V., et al. "Breakthrough in Mars balloon technology." *Advances in Space Research* 33.10 (2004): 1836-1841.

[11] Kremnev, R. S., et al. "VEGA balloon system and instrumentation." *Science* 231.4744 (1986): 1408-1411.

[12] Lorenz, Ralph D. "A review of balloon concepts for Titan." *Journal of the British Interplanetary Society* 61.1 (2008): 2

[13] Hall, Jeffery. "A survey of titan balloon concepts and technology status." *11th AIAA Aviation Technology, Integration, and Operations (ATIO) Conference, including the AIAA Balloon Systems Conference and 19th AIAA Lighter-Than*. 2011.

[14] MAVEN/NGIMS Thermospheric Neutral Wind Observations: Interpretation Using the M-GITM General Circulation Model

[15] Ringrose, T. J., M. C. Towner, and J. C. Zarnecki. "Convective vortices on Mars: a reanalysis of Viking Lander 2 meteorological data, sols 1–60." *Icarus* 163.1 (2003): 78-87.

[16] Farley, R., "BalloonAscent: 3-D simulation tool for the ascent and float of high-altitude balloons, AIAA 5th ATIO and 16th Lighter-Than-Air Sys Tech. and Balloon Systems Conferences, 2005, p. 7412.

[17] Appelbaum, J., and Landis, G. A., "Solar radiation on Mars: Update 1991," 1991.

[18] H. Kalita, R. T. Nallapu, A. Warren, J. Thangavelautham, "GNC of the SphereX Robot for Extreme Environment Exploration on Mars," Advances in the Astronautical Science, February 2017

[19] LeMaster, Edward A., and Stephen M. Rock. "A local-area GPS pseudolite-based navigation system for mars rovers." *Autonomous Robots* 14.2-3 (2003): 209-224.